NASA Technical Memorandum 118867

Moving Base Simulation of an Integrated Flight and Propulsion Control System for an Ejector-Augmentor STOVL Aircraft in Hover

Walter E. McNeill, William W. Chung, and
Michael W. Stortz

June1995

National Aeronautics and
Space Administration

NASA Technical Memorandum 108867

Moving Base Simulation of an Integrated Flight and Propulsion Control System for an Ejector-Augmentor STOVL Aircraft in Hover

Walter E. McNeill, William W. Chung, and Michael W. Stortz
Ames Research Center, Moffett Field, California

June 1995

National Aeronautics and
Space Administration

Ames Research Center
Moffett Field, CA 94035-1000

Nomenclature

b	wing span, ft
$\bar{c}$	wing mean aerodynamic chord, ft
$\Delta C_{l,\delta a}$	incremental rolling moment coefficient due to aileron deflection
$\Delta C_{m,\delta e}$	incremental pitching moment coefficient due to elevator deflection
$\Delta C_{n,\delta r}$	incremental yawing moment coefficient due to rudder deflection
F_{cmd}	commanded nozzle thrust, lbf
I_{xx}	moment of inertia about the X-body axis, slug-ft^2
I_{yy}	moment of inertia about the Y-body axis, slug-ft^2
I_{zz}	moment of inertia about the Z-body axis, slug-ft^2
L_{ps}	total rolling moment due to propulsion system and RCS thrusts, lbf-ft
M_{ps}	total pitching moment due to propulsion system and RCS thrusts, lbf-ft
N_{ps}	total yawing moment due to propulsion system and RCS thrusts, lbf-ft
$\dot{p}_{B,C}$	roll angular acceleration about the X-body axis due to ailerons and RCS nozzle thrusts, rad/sec^2
$\bar{q}$	dynamic pressure, $\rho V^2/2$, lbf/ft^2
$\dot{q}_{B,C}$	pitch angular acceleration about the Y-body axis due to elevators and RCS nozzle thrusts, rad/sec^2
$\dot{r}_{B,C}$	yaw angular acceleration about the Z-body axis due to rudder and RCS nozzle thrusts, rad/sec^2
S	wing reference area, ft^2
T_{2D}	2DCD (aft) nozzle thrust, lbf
T_{EJ}	ejector thrust, lbf
T_{VN}	ventral nozzle thrust, lbf
V	true airspeed, ft/sec
V_s	ship speed, knots
V_{wind}	wind velocity with respect to Earth reference, knots
V_{WOD}	wind velocity with respect to ship reference, knots
$\hat{y}_{ac}$	generalized aircraft state variable
y_{ac}	generalized state variable output of sensor compensation
y_{CMD}	generalized state variable command output of the Maneuver Command Generator
y_ε	generalized state variable error (input to Regulator)
δ^*	generalized actuator command (output of Regulator)
δ_{ac}	aerodynamic control actuator deflection, deg
$\delta_{ac,cmd}$	commanded aerodynamic control actuator deflection, deg
δ_a	aileron deflection, $(\delta_{e,R} - \delta_{e,L})/2$, deg
δ_e	elevator deflection, $(\delta_{e,R} + \delta_{e,L})/2$, deg
$\delta_{e,L}$	left elevon deflection, deg
$\delta_{e,R}$	right elevon deflection, deg
δ_r	rudder deflection, deg
θ_{cmd}	commanded thrust nozzle position, deg
ρ	air density, slugs/ft^3
ψ_{wind}	wind direction with respect to Earth reference, deg
ψ_{WOD}	wind direction with respect to ship reference, deg

Abbreviations and Acronyms

CG	center of gravity
CLM	component-level model
CMG	Configuration Management Generator
DMICS	Design Methods for Integrated Control Systems
FCS	flight control system
GEAE	General Electric Aircraft Engines
HPT	High-Pressure Turbine
HQR	handling qualities rating
HUD	head-up display
IFPCS	integrated flight and propulsion control system
IGV	Inlet Guide Vanes
LFWC	Lockheed Fort Worth Company
LPT	Low-Pressure Turbine
LQR	linear quadratic regulator
MCG	Maneuver Command Generator
MRC	moment reference center
PIO	pilot-induced oscillation
RCS	reaction control system
rms	root mean square
RTM	rapid thrust modulation
SKP	station-keeping point
STOVL	short takeoff, vertical landing
TDP	touchdown point
VMS	Vertical Motion Simulator (Ames)
V/STOL	vertical and/or short takeoff and landing
VSV	Variable Stator Vanes
2DCD	Two-Dimensional Convergent-Divergent

Moving Base Simulation of an Integrated Flight and Propulsion Control System for an Ejector-Augmentor STOVL Aircraft in Hover

WALTER E. MCNEILL, WILLIAM W. CHUNG, AND MICHAEL W. STORTZ

Ames Research Center

Summary

A piloted motion simulator evaluation, using the NASA Ames Vertical Motion Simulator, was conducted in support of a NASA Lewis contractual study of the integration of flight and propulsion systems of a short takeoff, vertical landing (STOVL) aircraft. Objectives of the study were to validate the Design Methods for Integrated Control Systems (DMICS) concept, to evaluate the handling qualities, and to assess control power usage. A highly nonlinear mathematical model of the E-7D ejector-augmentor STOVL fighter design and a component-level propulsion system model served as the basis for the simulation. On the basis of preliminary fixed-base evaluation, wherein the design was seen not to be completely developed over the full-flight envelope, motion simulation was restricted to hover and landing; all results and conclusions are limited to that flight phase.

The closed-loop response of the E-7D with integrated flight- and propulsion-control system (IFPCS), which was designed following the DMICS procedure, exhibited deficiencies which warrant further improvement of the design process to fully validate the DMICS concept.

With or without disturbances, handling qualities ratings (HQR) for the precision hover and shipboard landing tasks varied from satisfactory to adequate. Roll control power usage data indicate that increasing MIL-F-83300 roll control power specifications for hover should be considered. Acceptable pilot workload appeared to be attainable with integration of flight and propulsion controls in the specified simulation environment; i.e., wind, turbulence, and task.

Introduction

In connection with existing cooperative programs involving NASA and the aeronautical research establishments of the United Kingdom and Canada to develop technology applicable to advanced short-takeoff, vertical landing (STOVL) aircraft, NASA's Lewis Research Center had entered into a contract with General Electric Aircraft Engines (GEAE) to study integration of flight and propulsion controls.

The main purpose of this effort was to validate Design Methods for Integrated Control Systems (DMICS) (ref. 1) applied to a specific aircraft configuration—in this case the E-7D, an ejector-augmentor powered-lift aircraft designed by Lockheed Fort Worth Company (LFWC), the subcontractor to GEAE for this study. In support of this combined activity, piloted simulations, both fixed and motion based, were conducted at NASA Ames Research Center. The motion simulation, using the Ames Vertical Motion Simulator (VMS), is the subject of this report. Other work by NASA on the subject of integrated flight and propulsion control was reported in reference 2.

A simulation of an earlier version of this configuration, the E-7A (differing from the E-7D in details of the propulsion system and utilizing a simplified engine model and a flight-control system not based on DMICS methodology), was reported in reference 3. Although the results of that evaluation indicated that generally adequate to satisfactory handling qualities could be achieved in transition and hover, the present simulation was conducted to explore the benefits of an integrated flight and propulsion system based on the hierarchical, decentralized methodology of DMICS. In addition to application of the DMICS approach, the E-7D simulation model included nonlinear aerodynamic data based largely on small-scale wind-tunnel tests, a sophisticated component-level engine model, and a propulsive-lift system utilizing mixed flow at the ejector, ventral nozzle, and cruise nozzle.

A secondary purpose of this study was to assess the effectiveness and pilot acceptance of different control-command combinations and sensitivities. Depending upon the particular phase of flight and the control mode being evaluated, the pilot used a particular cockpit control, or inceptor, to command a given state variable (e.g., longitudinal stick force to command rate of change of flightpath angle or vertical velocity and throttle displacement to command longitudinal acceleration or longitudinal velocity). Since these inceptors more nearly resembled those for a conventional fighter airplane as opposed to a

powered-lift aircraft, and because all control effector positions were determined by the integrated flight- and propulsion-control system (IFPCS), reduced pilot workload was expected to be a benefit.

The purpose of this document is to report the results of the VMS motion simulation in terms of pilot evaluations of the handling qualities, cockpit controls, and control-power availability in precision-hover and shipboard landing tasks. The state of IFPCS development for the E-7D at the time of the present piloted simulation evaluation allowed simulator motion to be used only in hover. Therefore, all discussion in this report of system performance and aircraft handling qualities is limited to that flight phase.

Aircraft Description

The E-7D design used as a basis for the present simulation study was developed by LFWC as a potential supersonic fighter/attack aircraft with an ejector-augmentor powered-lift system to provide STOVL capability. This design differs from the earlier E-7A (ref. 3) mainly in the propulsion- and flight-control systems. The E-7A employed split flow, where fan air was ducted to the ejectors and to the aft nozzle and core flow was routed to a vectorable ventral nozzle; the E-7D propulsion system utilized mixed fan and core flow to all three thrust nozzles (counting the ejectors as one). Air flow for the reaction control system (RCS) was supplied by bleed from the high-pressure compressor. The E-7D flight control system (FCS) was developed as part of an integrated flight- and propulsion-control system (IFPCS) based on a hierarchical, decentralized methodology known as DMICS. DMICS uses modern control system design techniques, such as state space and optimal control theories, to optimize control power usage throughout the flight envelope. The earlier E-7A FCS was designed using nonlinear inverse methods, which solve the aerodynamic and propulsive control commands directly from the pilot control commands (flightpath or velocity).

Basic Aircraft

Figure 1 shows the general arrangement of the E-7D. The fuselage, cockpit, and vertical tail were those of the single-seat F-16. The overall configuration was that of a tailless delta wing with a leading-edge sweep of 60 deg. Table 1 presents dimensional data critical to the present simulation. Table 2 shows pertinent weight and inertia data.

Aerodynamic data for the E-7D simulation mathematical model were derived from several sources: Clean configuration static data from wind-tunnel tests of a 1/9-scale E-7A model (ref. 4), power-induced aerodynamics (with ejector doors open) from tests of a 30 percent-scale powered model (ref. 5), RCS-induced and power-induced aerodynamics from a 15 percent-scale free-flight model (refs. 6 and 7), and power-induced ground effects, such as suckdown, from the 15 percent-scale model configured for hover (unpublished data). Dynamic stability derivatives were estimated for low angles of attack by application of the USAF Stability and Control DATCOM (ref. 8), extended to high angles of attack via trends shown by F-16XL and/or B-58 data. Landing gear aerodynamic effects were derived from F-16 data.

Propulsion System

The propulsion system was designed around a derivative of the General Electric Aircraft Engines (GEAE) F110 turbofan engine, sized to meet the requirements of the E-7D. Maximum gross thrust was approximately 19,000 lbf. In addition to a two-dimensional convergent-divergent (2-DCD) vectorable aft nozzle for up-and-away flight, the powered-lift system comprised two sets of ejector nozzles mounted in the wing close to the fuselage and a vectorable ventral nozzle for pitch balance and fore/aft control in hover. Air flow to all ports (except the RCS) consisted of mixed fan and core flow. A maximum of 7 percent of the compressor discharge flow was available to the RCS. Figures 2 and 3 show the arrangement of the components of the propulsion system.

The ejectors were fitted with upper and lower doors, which were closed and faired during cruise flight. For powered-lift flight (transition and hover) both sets of doors were open, providing an ejector thrust augmentation ratio of 1.7. Ejector thrust modulation was accomplished by means of the butterfly valve, and ventral nozzle thrust was varied by a set of shutters, which were closed for cruise flight. The 2-DCD nozzle was closed completely during hover operation.

For simulation purposes, a component-level model (CLM) of the propulsion system was developed by GEAE (ref. 9). The model contained each major engine component, including inlet, fan and low-pressure compressor, high-pressure compressor, bypass duct, main burner, high-pressure turbine, low-pressure turbine, bypass and core flow mixing, and calculation of individual nozzle thrusts, as well as a propulsion-control system with a multivariable regulator and rapid thrust modulation (RTM) by means of variable stator vanes. The propulsion

system was designed to meet small and large magnitude thrust response specifications generated by LFWC.

Maximum core mass flow rate was 250 lbm/sec; maximum RCS thrusts (per nozzle) were: roll, 400 lbf; pitch, 300 lbf; yaw, 500 lbf. Nominal thrust split was 40 percent ejectors, 60 percent ventral nozzle. In general, the propulsion system response bandwidth was 10 rad/sec.

Flight Control System

The E-7D STOVL FCS consisted of six major components (fig. 4) which were the Maneuver Command Generator (MCG), Configuration Management Generator (CMG), Regulator, Control Selector, Actuators, and Sensor Compensation. The control system design employed explicit model following with proportional and integral gains, developed by Linear Quadratic Regulator (LQR) synthesis about six selected design points: two in cruise, two in transition, and two in hover. A detailed description of the FCS and its integration with the propulsion system is given in reference 9.

The MCG handled the control mode selection made by the pilot, shaped the pilot control inputs, and generated mission-level control commands (i.e., flightpath or velocity commands in response to pilot control commands). For design purposes, the flight envelope was divided into three flight modes: cruise, transition, and hover. In cruise the pilot commanded aft nozzle thrust, roll rate, pitch rate and sideslip. In transition the pilot commanded longitudinal acceleration, roll rate, vertical flightpath (or flightpath rate) and sideslip. In hover (the only flight mode for which results are presented here), the pilot commanded longitudinal velocity, roll rate, vertical velocity, and lateral velocity. The relationship of inceptors to commanded variables is described in the Simulation Experiment section under Experiment Configurations. Washout circuits were included to smooth the transient response when switching between flight modes. Second-order command generators were customized to meet mission-level handling qualities specifications for STOVL aircraft in this class.

The CMG defined the propulsion system trim states for the regulator based on the specific flight configuration, such as wing-borne with landing gear up, wing-borne with landing gear down, approach, hover, and on-ground operation. The trim thrusts and nozzle positions were scheduled as functions of airspeed and flightpath angle. The trim schedule was developed to minimize abrupt and large amplitude thrust changes and attitude transients due to these thrust changes.

The Regulator produced generalized actuator commands to achieve model following characteristics and control stability with respect to MCG control commands. The regulator was designed based on linearized aircraft stability derivatives and linear quadratic formulations with output error weightings. Proportional plus integral control was used to ensure zero steady-state error.

The Control Selector converted generalized actuator commands to physical actuator commands, which included aerodynamic control surfaces, propulsive thrusts, and nozzle deflections. Pseudo-inverse transformation was used to make this conversion, since the number of physical control actuators was greater than that of the generalized actuator commands. Each physical control was weighted based on its effectiveness during the transformation. The pitch axis generalized actuator command distribution was given higher priority than were the longitudinal and vertical command degrees of freedom. The Hanus anti-windup algorithm (ref. 10) was used to protect system stability in the presence of the nonlinear characteristics of the physical actuators. The unmet generalized actuator commands were fed back to the MCG to condition the control commands so that the generalized actuator commands would always stay within the physical actuators' linear bounds.

The Actuators contained the dynamics of all aerodynamic surfaces, reaction control system area control valves, ejector doors, and landing gear extension/retraction. All actuator dynamics were simulated with first-order transfer functions with appropriate time constants, rate limits, and position limits.

The Sensor Compensation provided aircraft states in inertial and body coordinates for the closed-loop feedback control. First-order filters with corresponding cut-off frequencies were used to remove high-frequency noise normally seen on the aircraft.

First-order complementary filters were employed to generate forward velocity and sideslip.

Simulation Experiment

A total of seven pilots took part in the simulator evaluation. All were highly trained and experienced test pilots. Five pilots represented NASA or its support contractors, while two were employed by LFWC. The only ones with extensive powered-lift flight experience were four of the NASA-affiliated pilots.

Simulation Facility

Ames Research Center's VMS (fig. 5) was used for the piloted evaluation. The VMS is a large-scale motion simulator coupled to a VAX 9000 digital computer and an

Evans and Sutherland CT5A visual scene generator. Complete descriptions of all components of the VMS system are given in reference 11. For the purpose of this experiment, the cab and angular-motion support were rotated 90 deg, so that the large motion along the beam became the longitudinal motion axis.

Figure 6 shows an interior view of the cockpit, including locations of the control inceptors. Figure 7 shows schematically the instrument panel layout. The three-window visual display provided a choice of reference targets for a precision hover task (fig. 8) or a small-ship (DD963) scene for shipboard approach and landing (fig. 9).

All pertinent flight information was presented in a head-up display (HUD), the details of which are shown in figure 10. The symbology and drive laws for this HUD were as described in reference 12, updated according to reference 13.

Evaluation Tasks and Procedures

In order to evaluate the E-7D handling qualities and IFPCS performance in hover, two different types of pilot tasks were used: (1) precision hover with reference to fixed targets (fig. 8) and (2) shipboard approaches and landings aboard a Spruance class destroyer (DD963, fig. 9). The Cooper-Harper handling qualities rating (HQR) scale (fig. 11) (ref. 14) was used to evaluate these tasks.

Figure 12 depicts the lateral and vertical precision hover tasks. For the lateral task, the airplane's initial position was 500 ft in front of the target array at a height of 50 ft. That position was established by setting the simulation initial conditions. From that position, the task was to translate to and stabilize at a position 90 ft in front of the right hand target, translate laterally and stabilize in front of the left hand target, then translate and stabilize again at the right hand target, all within a time limit of 55 sec. The 90-ft distance and the lateral/vertical position at each target were established visually according to the sight picture illustrated in figure 8(c), where the "rabbit ears" appear to form a continuous horizontal bar, the corners of which match the inside corners of the end squares on the backboard. Allowable deviations for desired and adequate performance were demonstrated visually to the pilot by statically positioning the eye point prior to performing the tasks.

For vertical precision hover, beginning at the same initial position, the task was to translate to and stabilize at a position 90 ft in front of the lower target, ascend to and stabilize in front of the upper target, then descend and stabilize again at the lower target, all within 75 sec. For the purpose of interpreting the Cooper-Harper rating scale and assigning a handling qualities rating, allowable errors were established corresponding to desired or adequate performance. These errors for the precision hover tasks are shown in figure 12.

Figure 13 depicts the shipboard landing task. From an initial height 50 ft above the landing deck and a position 400 ft directly aft of the station-keeping point (SKP), which itself was 100 ft aft and 100 ft to port of the landing deck touchdown point (TDP), the task was to translate forward at a constant height to the SKP (which was always fixed with respect to the ship axes), stabilize there, then translate to a point directly over the TDP and descend to the deck. The deck landing area was 40 ft by 70 ft. The target time from the SKP to touchdown was 35 sec. The normal descent rate with respect to the deck was approximately 4 fps. Allowable touchdown errors for desired or adequate performance are also shown in figure 13.

Of the seven pilots who took part in the simulator evaluation, Pilots A, B, C, and G had extensive background and experience in jet-lift and other vertical and/or short take-off and landing (V/STOL) aircraft. Those with V/STOL shipboard experience were pilots A and C. Pilots D, E, and F had considerable military experience in conventional fighters. Pilots B and G did not formally evaluate the precision hover tasks; all pilots evaluated the shipboard landing task.

Experiment Configurations

The experiment variables of concern in this simulation were divided into two control system configurations and either two or four disturbance conditions, depending on whether precision hover or shipboard landing tasks were being performed.

Figure 14 shows the control-inceptor/command-variable relationships for the "front-side" and "back-side" control modes. All three flight phases (cruise, transition, and hover) are included for clarity and completeness, though only hover was evaluated formally. The front-side mode was so called because the manner of control was similar to that of an airplane on the front side of the power curve; that is, forward acceleration or velocity was controlled by throttle movement and flightpath angle or vertical velocity was controlled with longitudinal stick. The back-side mode owed its name to the technique used on the back side of the power curve, where flightpath or vertical velocity was commanded with the left-hand controller (the throttle) and pitch attitude (and consequently forward velocity) was controlled using longitudinal stick. In the present experiment using the back-side mode, forward

acceleration with velocity hold in the transition phase was commanded with a thumbwheel (the antenna elevation knob) on the throttle grip and, in hover, longitudinal velocity was commanded with longitudinal stick force. Switches and buttons available for trimming the commanded variables are also shown in figure 14. Figure 15 shows the longitudinal and lateral force vs. deflection characteristics of the right-hand controller. This controller, from an F-16, had very limited motion and is referred to hereinafter as the right-hand force controller or force stick.

Table 3 shows the disturbance conditions used in the experiment. Ambient wind velocity and direction are indicated for the precision hover task, with the forward-aft axis of the hover targets on a heading of 163 deg. For the shipboard landing task, both ambient wind and wind over the deck are shown, as well as ship speed and sea state. Basic standards for specifying these disturbance conditions were obtained from reference 15.

Results and Discussion

Handling Qualities Evaluation

Precision hover– HQRs for the precision hover tasks are presented individually for pilots A, C, D, E, and F in table 4 and are also plotted in figure 16. The data are broken down into lateral task and vertical task for the front-side and back-side control modes, for two atmospheric conditions: calm air and a 15 knot wind at 30 deg from the left forward quarter with a turbulence level of 6 fps root mean square (rms).

For the lateral task in calm air, the E-7D simulation using the front-side control mode was consistently rated as satisfactory, or Level 1. All other combinations for the lateral task were distributed between Level 1 and Level 2 (adequate). (A complete discussion of Levels of flying qualities and their relation to HQRs are presented in ref. 16.) For the front-side mode, the HQRs given by pilots D, E, and F, whose backgrounds were in conventional non-powered-lift fighters and who stated that their training and experience made the front-side mode more natural to them (i.e., similar to the technique used in formation flying or aerial refueling, wherein longitudinal position is controlled with throttle and vertical position by longitudinal stick) were consistently more favorable than those given by pilots A and C. Pilots A and C had extensive V/STOL experience, where during low-speed and hover operation the use of throttle to control vertical velocity and right-hand center or side stick to control translational velocity in the horizontal (X-Y) plane was the normal technique. For this reason the back-side mode was more natural to them.

Except for pilots C and D, HQRs for the back-side mode in the lateral task for both calm and disturbed conditions were less favorable than for the front-side mode, in three cases moving from Level 1 to Level 2 (notably with pilot E). This difference was generally due to difficulty establishing desired longitudinal position aggressively, using the right-hand force controller. This controller received many complaints regarding high force gradients and almost no inceptor position feedback to the pilot, causing a lack of smoothness of response (described as "ratchetiness"), mostly in longitudinal translation.

For the vertical task, as for the lateral task, using the front-side mode (fig. 16), the HQRs from the non-V/STOL pilots were more favorable than those from the V/STOL pilots, again demonstrating the difference in acceptance of the front-side technique as it is influenced by differences in training and experience. The most unfavorable ratings fell deep in the Level 2 region. The major factors driving these Level 2 ratings were imprecise control of heading and difficulty coordinating lateral and directional control inputs during the initial horizontal translation to the vertical targets, cross-axis coupling (lateral into vertical) introduced using the right-hand force controller, and the need to coordinate left-hand throttle inputs (for forward translation) and right-hand lateral inputs to arrive at the desired position in front of the vertical targets. Some difficulty capturing the upper vertical target was also reported if the pilot used moderately aggressive vertical inputs; some pilot-induced oscillation (PIO) tendencies were seen, attributed to a somewhat long apparent time constant in the vertical response combined with the characteristics of the right-hand force controller. In contrast, pilot F, who consistently rated this task/control-mode combination Level 1, reported no adverse characteristics other than a little cross-axis control coupling with the force stick.

In corresponding atmospheric conditions, the vertical task using the front-side mode was generally rated less favorably than the lateral task, partly because of the more extensive maneuver required to reach the necessary X-Y position in front of the vertical targets. The apparent long time constant of the vertical response, mentioned in the preceding paragraph, was also a factor.

The vertical task using the back-side control mode was rated consistently at 4.0. The principal reason for not rating these cases better than Level 2 was the persistent difficulty capturing precisely a desired longitudinal position using the force stick. Good height control using throttle displacement and relative ease of control of X-Y position with a single controller, however, were reported.

On average, for these tasks using the front-side mode, the presence of wind and turbulence required enough

additional pilot compensation to cause a deterioration of about one HQR. In the back-side mode, there was no influence of wind and turbulence on the ratings.

Shipboard landing– HQRs for the shipboard landing task are presented for pilots A through G in table 5. Figure 17 presents these data plotted for zero ship speed and as a function of sea state and wind condition for a ship speed of 10 knots.

In calm conditions and with zero ship speed, the front-side control mode showed a division between V/STOL and non-V/STOL pilots similar to that observed during the precision hover tasks, though to a lesser degree, the average HQR for the non-V/STOL pilots being just one rating point more favorable. Without disturbances of any kind, performance of the task with the front-side mode was generally considered not difficult. Longitudinal velocity control using the throttle was considered good to excellent. Where the HQRs were not better than Level 2, the pilots complained of the workload associated with coordination between the left-hand and right-hand controllers when maneuvering in the X-Y plane, and of inadvertent cross-axis inputs using the right-hand force controller (usually lateral control coupling into vertical).

For the front-side mode, the effect of added disturbances on HQRs appeared to be largely due to the ship speed of 10 knots, with the increased sea state (and to some extent wind and turbulence level) increasing the HQR spread into the Level 3 region. Being a displacement controller, the throttle was found to be an effective means of commanding forward velocity to match that of the ship (i.e., the station-keeping point), almost lending itself to a "set and forget" operation. For these cases, some pilots continued to comment adversely on the need for left-hand/right-hand coordination as well as cross-axis contamination using the force stick. Additional complaints were also noted regarding the force stick. These were lack of precision and smoothness of response (traceable to force gradient or command sensitivity) and the need to hold lateral stick force to match the ship velocity with the aircraft heading into the wind, from 30 deg left of the bow. There was a provision for trimming out the force, but the requirement to release force on the stick grip in order to do so made that difficult. A similar problem was encountered when attempting to trim out longitudinal force in the back-side control mode, discussed in the following paragraphs.

For the back-side control mode in calm conditions, the overall average HQR was a small fraction of a rating point more favorable than for the front-side mode. The division in average HQR according to pilot background was also present for the back-side mode, but to a much smaller degree than for the front-side mode. Control of height using the throttle controller was considered good to excellent.

The addition of ship speed, sea state, and wind and turbulence had an effect on mean level and spread of HQRs similar to that observed for the front-side mode (fig. 17). In the more severe conditions (sea state 3 and 4 plus wind and turbulence) the majority of the pilots rated the back-side mode equal to or better than the front-side mode; the one exception was one of the non-V/STOL pilots, pilot F, who consistently tended to favor the front-side mode for all tasks. The good vertical-velocity control using the throttle controller carried over into these disturbed cases.

For the back-side mode at sea state 4, a wide discrepancy in HQR was noted between pilots A and B. Landing performance (touchdown position error and vertical velocity) was within desired limits for both pilots. Pilot A complained of excessive workload in compensating for that amount of deck motion, coupled with difficulty making small, precise inputs using the force stick, whereas pilot B considered the workload minimal and described the maneuver from the SKP to touchdown as "not too bad." Both pilots did report difficulty using the longitudinal trim button on the force stick to relieve the steady forward force required to approach the SKP and match the ship's velocity. When actuating the trim button with the thumb, it was necessary momentarily to relax hand pressure on the stick, resulting in an unsteady approach to the SKP. This initial phase, however, was not part of the formal evaluation task and was not used in arriving at the HQRs.

The vast majority of comments on the back-side mode were regarding the right-hand force controller and the manner in which it was integrated into the control system. At least three of the other pilots (not just A and B) found the need to hold force to match ship speed troublesome unless trimmed out. As mentioned earlier, the method of trimming provided was not entirely satisfactory.

Other drawbacks of the force controller installation that were mentioned were force gradient or sensitivity problems similar to those encountered in the front-side mode, leading to imprecise and "ratchety" control response, and unwanted cross-axis inputs (this time in the X-Y plane). A more optimal orientation of the force controller unit in the cockpit could have alleviated some of the latter problem.

Both the front-side and back-side modes were evaluated by pilots A and C, and the back side by pilot D, in 20 ft visibility and zero ceiling, with ship speed of 10 knots and sea state zero (fig. 17). These cases were given an HQR of 5, the same as for unlimited visibility, the pilots citing the same control deficiencies as before, with minimal effect of reduced visibility. Even with unlimited visibility, these pilots relied mainly on the HUD for rate and position

guidance. In the restricted visibility cases, the HUD was the sole source for rate and position guidance.

Because it lent itself readily to the task, all pilots relied to some degree on the HUD hover mode for guidance to the touchdown point and descent to landing. The degree to which each was able to use the HUD depended on his familiarity with the symbology. Pilots A, B, C, and G had the most experience with this display, in this and previous STOVL simulations. Pilots D, E and F had prior experience with the display only during the fixed-base exercise leading to the present simulation in the VMS and, consequently, less HUD familiarity coupled with relative lack of V/STOL experience. Since there was insufficient time to bring these latter three pilots to a level comparable with that of pilots A, B, C, and G some adverse effect on their ratings would be expected.

To sum up the piloted evaluation, the following statements can be made: For the precision hover tasks, HQRs (considering both front-side and back-side control) were spread over a range covering Level 1 and Level 2, with more ratings falling in the Level 2 range in the presence of moderate wind and turbulence. For the shipboard landing task with zero ship speed, no deck motion and no wind and turbulence, HQRs covered the same range (Level 1 and Level 2) as for precision hover. The addition of 10 knots of ship speed resulted in Level 2 ratings in practically every case; the further addition of deck motion, and moderate wind and turbulence increased the HQR spread within the Level 2 range and even beyond. Single-axis response, with exception of the yaw axis, did not cause great problems; however, cross-coupling effects were often present which were annoying or even unsatisfactory. Yaw control was characterized by an apparent long time constant which, in combination with absence of a heading-hold loop, made capture of a desired heading difficult. Several pilots (notably pilots A and C) found the right-hand force controller difficult to use and unsuitable for jetborne flying tasks. Objectionable characteristics were found in the rudder pedals, attributed to their also being force controllers. For jetborne maneuvering, those pilots highly experienced in V/STOL operations (A, B, C, and G) expressed a clear and sometimes forceful preference for the back-side control mode, wherein vertical velocity was commanded with a left-hand controller and longitudinal and lateral velocities were commanded by means of a single right-hand controller.

Control Power Usage

The control power has direct consequence to the trimming, maneuvering, and stabilization of the aircraft in any flight condition. The control response requirements for V/STOL, in terms of attitude change in one second, have been specified by MIL-F-83300 (ref. 16) and AGARD R-577-70 (ref. 17) for hover and low speed flight operations. In reference 18 these specifications have been related to control power and compared with later experimental data. These comparisons suggest that the roll control response specified in references 16 and 17 may not be adequate for shipboard landings in severe weather conditions. One of the objectives of the present experiment, therefore, was to examine the control power usage requirements for the E-7D STOVL aircraft in adverse weather conditions.

The control power usage is contributed by both the aerodynamic control effectors and the propulsive thrusts. The roll, pitch, and yaw control power usage for this experiment were calculated as follows:

$$\dot{p}_{B,C} = \left(\bar{q}SbC_{\ell,\delta_a} + L_{PS}\right)\Big/I_{xx}$$

$$\dot{q}_{B,C} = \left(\bar{q}S\bar{c}C_{m,\delta_e} + M_{PS}\right)\Big/I_{yy}$$

$$\dot{r}_{B,C} = \left(\bar{q}SbC_{n,\delta_r} + N_{PS}\right)\Big/I_{zz}$$

The control power usage in the shipboard landing task for various weather and sea state conditions is shown in figure 18. It is shown that the roll control power usage in both calm air and adverse weather conditions has exceeded MIL-F-83300 control power requirement for 2 rad/sec attitude system with a damping ratio of 0.8944 (ref. 18). The pitch control power usage in adverse weather condition has also exceeded the specified requirement for a 2 rad/sec rate system.

Conclusions

A piloted motion simulator evaluation was completed in support of a contractual study of the integration of flight and propulsion controls of a short takeoff, vertical landing (STOVL) aircraft. The objectives of the study were to validate the Design Methods for Integrated Control Systems (DMICS) concept, to evaluate the handling qualities, and to assess control power usage during hover and landing. From this evaluation the following conclusions are drawn:

1. The closed-loop response of the E-7D with the integrated flight- and propulsion-control system (IFPCS), which was designed following the DMICS procedure, exhibited deficiencies which warrant further improvement of the design process to fully validate the DMICS concept.

2. With mild to moderate wind and turbulence, using either the front-side or back-side control mode, handling qualities were judged to be adequate (Level 2) to

marginally satisfactory for the precision hover tasks. Under similar atmospheric conditions and with 10 knots of ship speed, both the front-side and back-side modes on average were rated Level 2 for the shipboard landing task. Increasing sea state to 3 and 4 resulted in a correspondingly greater spread of ratings.

3. Roll control power usage data indicate that increasing MIL-F-83300 roll control power specifications for hover operations should be considered. Further experiment is required to determine if MIL-F-83300 pitch control power specification is adequate.

4. With no disturbances, using the front-side control mode, average handling qualities ratings (HQR) were in the satisfactory region (Level 1) both for the precision hover and shipboard landing tasks. In the same conditions, using the back-side control mode, average handling qualities ratings were borderline Level 1/Level 2 for the lateral precision hover task, Level 2 for the vertical precision hover task, and Level 1 for the shipboard landing task.

5. In the front-side or back-side mode, use of the limited-displacement force controller (the right-hand side stick) for maneuvering in hover resulted in objectionably high pilot workload.

References

1. Shaw, P. D. et al: Design Methods for Integrated Control Systems. AFWAL-TR-88-2061, June 1988.

2. Garg, Sanjay; Ouzts, Peter J.; Lorenzo, Carl F.; and Mattern, Duane L.: IMPAC—An Integrated Methodology for Propulsion and Airframe Control. NASA TM-103805, June 1991.

3. Franklin, James A.; Stortz, Michael W.; Gerdes, Ronald M.; Hardy, Gordon H.; Martin, James L.; and Engelland, Shawn A.: Simulation Evaluation of Transition and Hover Flying Qualities of the E-7A STOVL Aircraft. NASA TM-101015, Aug. 1988.

4. Foley, W. H.; Albright, A. E.; Powers, D. J.; and Smith, C. W.: Study of Aerodynamic Technology for Single-Cruise-Engine V/STOL Fighter/Attack Aircraft, Phase II Final Report, Volumes I and II. NASA CR-177367, Aug. 1985.

5. Banks, Daniel W.; and Gatlin, Gregory M.: Longitudinal and Lateral Aerodynamic Data from Tests of an Advanced STOVL Fighter Employing a Powered- Lift Ejector. NASA TM-87672, May 1986.

6. Riley, Donald R.; Shah, Gautam H.; and Kuhn, Richard E.: Low-Speed Wind-Tunnel Study of Reaction Control-Jet Effectiveness for Hover and Transition of a STOVL Fighter Concept. NASA TM-4147, Dec. 1989.

7. Riley, Donald R.; Shah, Gautam H.; and Kuhn, Richard E.: Some Power-Induced Effects for Transition Flight Measured on a 15-Percent Scale E-7A STOVL Fighter Model. NASA TM-4188, June 1990.

8. Williams, J. E.; and Vukelich, S. R.: The USAF Stability and Control Digital DATCOM, Volumes I, II and III. AFFDL-TR-79-3032, Apr. 1979.

9. Adibhatla, S.; Cooker, P.; Pajakowski, A.; Romine, B.; Virnig, J.; and Bodden, D.: STOVL Controls Technology, Volumes I, II, and III. NASA CR-195361, July 1994.

10. Hanus, R.; Kinnaert, M.; and Henrotte, J. L.: Conditioning Technique—A General Anti-Windup and Bumpless Transfer Method. Automatica, vol. 23, no. 6, Nov. 1987, pp. 729–739.

11. Danek, George: Vertical Motion Simulator Familiarization Guide. NASA TM-103923, Oct. 1991.

12. Merrick, Vernon K.; Farris, Glenn G.; and Vanags, Andrejs A.: A Head Up Display for Application to V/STOL Aircraft Approach and Landing. NASA TM-102216, Jan. 1990.

13. Merrick, Vernon K.: Some VTOL Head-Up Display Drive-Law Problems and Solutions. NASA TM-104027, Nov. 1993.

14. Cooper, George E.; and Harper, Robert P., Jr.: The Use of Pilot Rating in the Evaluation of Aircraft Handling Qualities. NASA TND-5153, Apr. 1969.

15. Fortenbaugh, Robert L.: Mathematical Models for the Aircraft Operational Environment of DD-963 Class Ships. Vought Corp. Rep. 2-55800/8R-3500, Sept. 1978.

16. Chalk, Charles R.; Key, David L.; Kroll, John, Jr.; Wasserman, Richard; and Radford, Robert C.: Background Information and User Guide for MIL-F-83300 Military Specification—Flying Qualities for Piloted V/STOL Aircraft. AFFDL-TR-70-88, Nov. 1971.

17. Anon.: V/STOL Landing, I – Criteria and Discussion. AGARD R-577-70, Dec. 1970.

18. Franklin, James A.: Criteria for Design of Integrated Flight/Propulsion Control Systems for STOVL Fighter Aircraft. NASA TP-3356, Apr. 1993.

Table 1. E-7D principal dimensions

Wing span, ft	32.4
Wing area, ft^2	630.6
Aspect ratio	1.66
Taper ratio	0.115
$\bar{c}$, ft	23.56
MRC, % $\bar{c}_w$	30.00
CG, % $\bar{c}_w$	35.97
$\delta_{eL,R}$ (max) deg	±30
δ_r (max) deg	±20

Table 2. Weight and moments of inertia (hover, landing gear down)

Weight, lb	17,000
I_{xx}, slug-ft^2	4,415
I_{yy}, slug-ft^2	29,413
I_{zz}, slug-ft^2	29,963
I_{xz}, slug-ft^2	–70.51

Table 3. Task environmental conditions

Wind condition	At hover targets with heading 163 deg			At ship with heading 000 deg						
	V_{wind}, kt	ψ_{wind}, deg	rms turb., fps	V_{wind}, kt	ψ_{wind}, deg	Ship speed, kt	V_{WOD}, kt	ψ_{WOD}, deg	rms turb., fps	Sea state
W1	0	0	0	0	0	0	0	0	0	0
W2	15	133	3	8.11	292	10	15.04	330	3	0
W2A	15	133	6	8.11	292	10	15.04	330	6	3
W2B	15	133	6	8.11	292	10	15.04	330	6	4

Visibility condition	Visual range, ft	Ceiling, ft
V1	Unlimited	Unlimited
V6	20	0

Table 4. HQRs for precision hover tasks[a]

Task	Lateral				Vertical			
Control mode	Frontside		Backside		Frontside		Backside	
Wind / Pilot	W1	W2A	W1	W2A	W1	W2A	W1	W2A
A	3	4	4	5	4	6	4	4
C	3	5	3	4	5	6	4	4
D	3	3	3	3	3	4	4	4
E	2	3	4.5	4.5	3	3	4	4
F	2	2	3	3	2	3	4	4

[a]Visibility: V1.

Table 5. HQRs for shipboard landing task

Control mode	Frontside				Backside			
Wind	W1	W2	W2A	W2B	W1	W2	W2A	W2B
Visibility / Pilot	V1	V1,V6	V1	V1	V1	V1,V6	V1	V1
A	4	5	6	7	4	5	5	7
B	3	—	4	4	3	—	—	3
C	5	5	5	6	3	5	5	6
D	3	—	5	6	4	—	5	5
E	4	—	4.5	5	3	—	4	4.5
F	2	—	5	5	2	—	6	6
G	3	—	6	6	2	—	4	5

Wing	
• **Area**	**630.6 ft^2**
• **Aspect ratio**	**1.665**
• **Taper ratio**	**0.115**
• **Airfoil**	**NACA 64A004**
• **t/c**	**4%**
Vertical tail	
• **Area**	**68.4 ft^2**
• **Aspect ratio**	**1.294**
• **Taper ratio**	**0.437**
• **Airfoil**	**Biconvex**

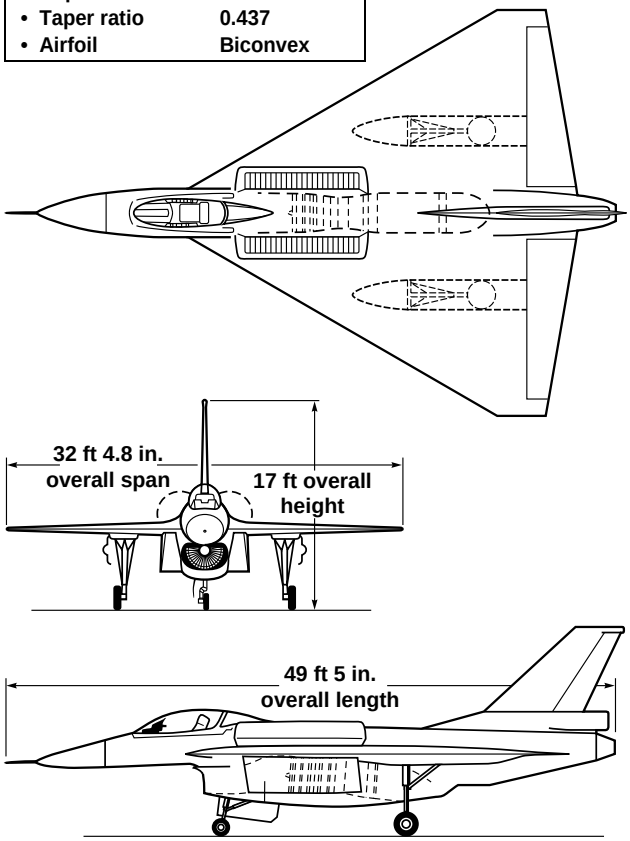

Figure 1. Three views of E-7D aircraft.

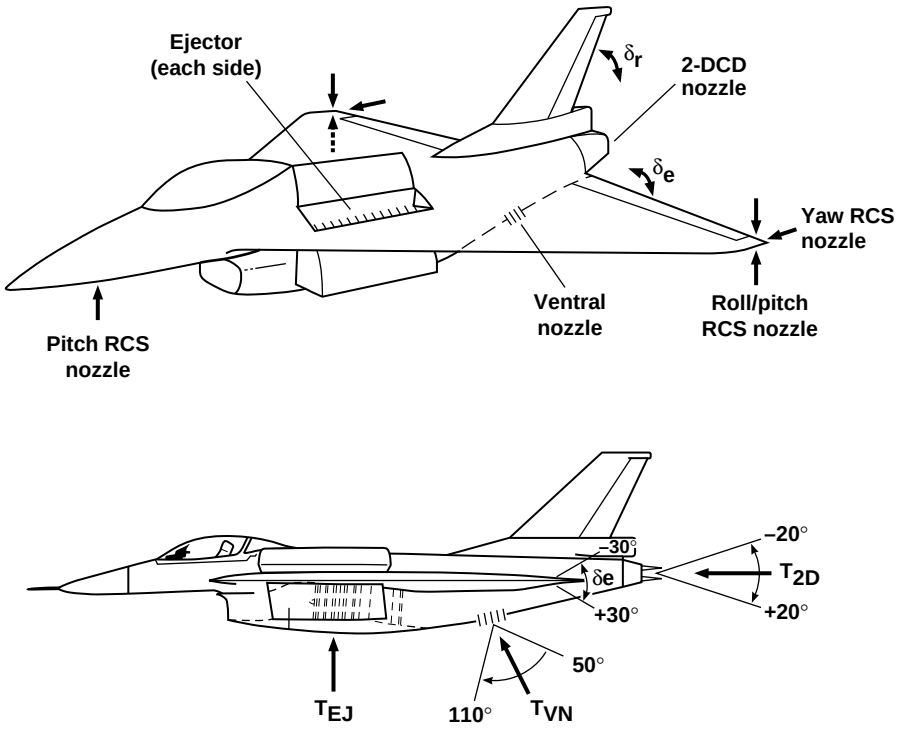

Figure 2. Arrangement of propulsive nozzles and RCS nozzles.

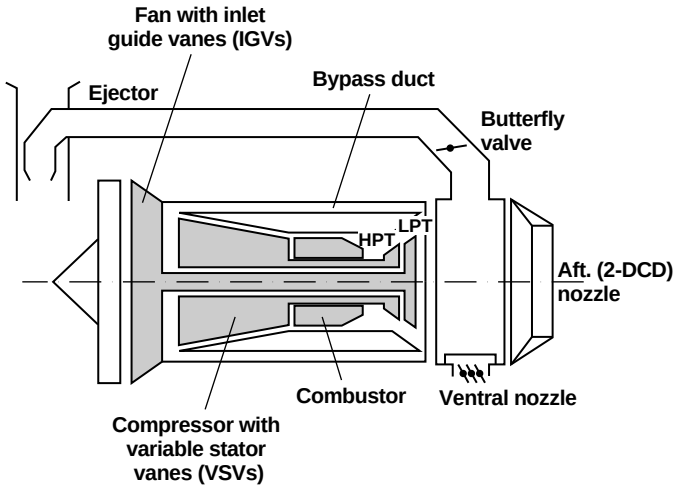

Figure 3. Propulsion system schematic diagram.

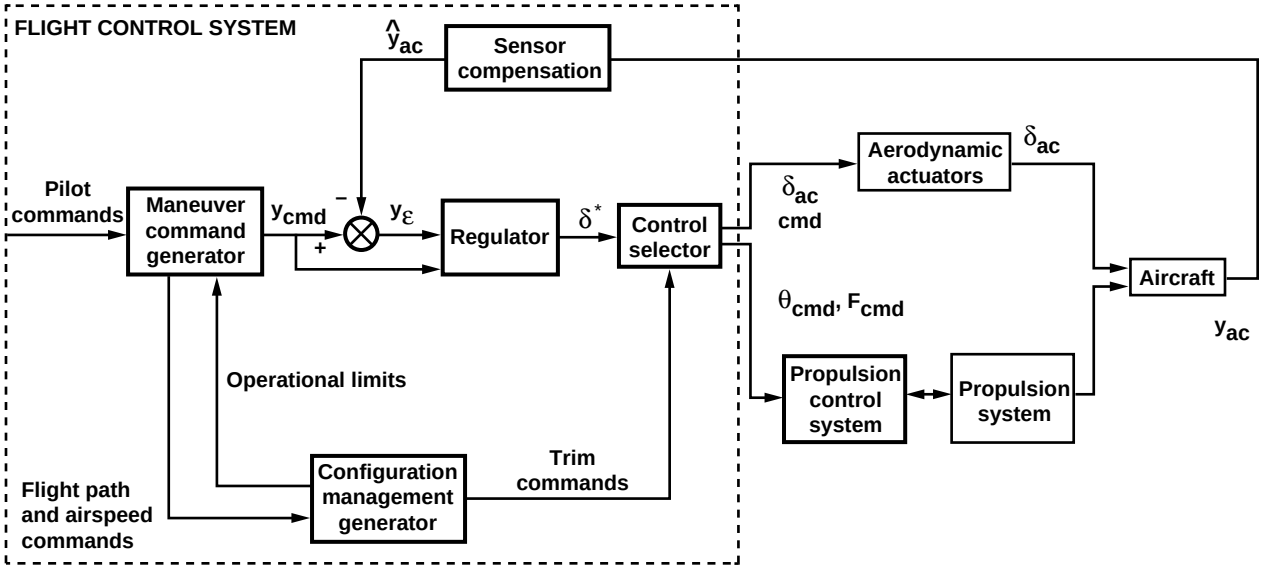

Figure 4. Integrated flight- and propulsion-control system structure.

VMS NOMINAL OPERATIONAL MOTION LIMITS			
Axis	**Displ**	**Velocity**	**Accel**
Vertical	**±30**	**16**	**24**
Lateral	**±20**	**8**	**16**
Longitudinal	**±4**	**4**	**10**
Roll	**±18**	**40**	**115**
Pitch	**±18**	**40**	**115**
Yaw	**±24**	**46**	**115**
All numbers, units in ft, deg, sec			

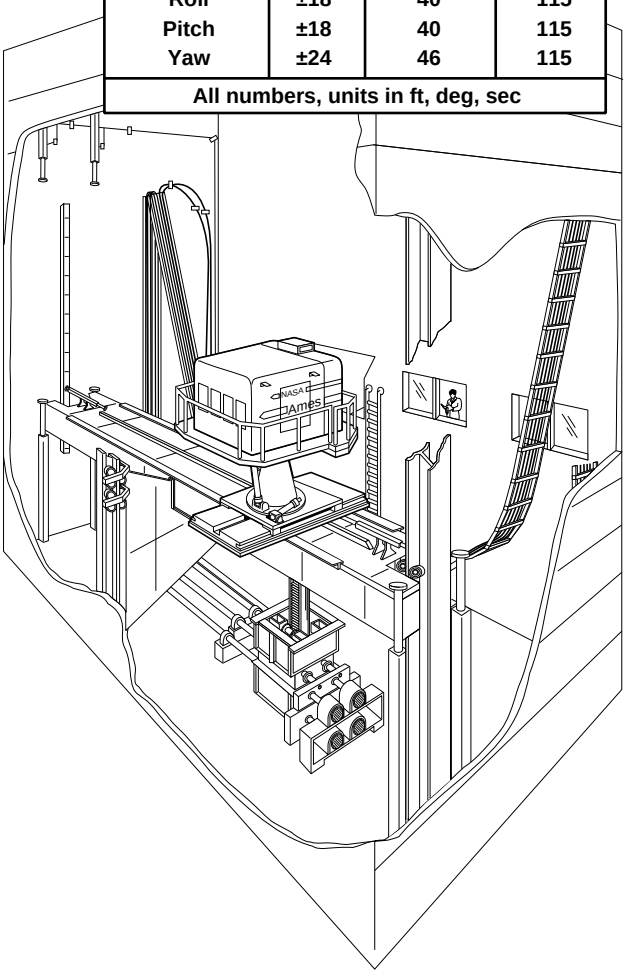

Figure 5. Vertical Motion Simulator.

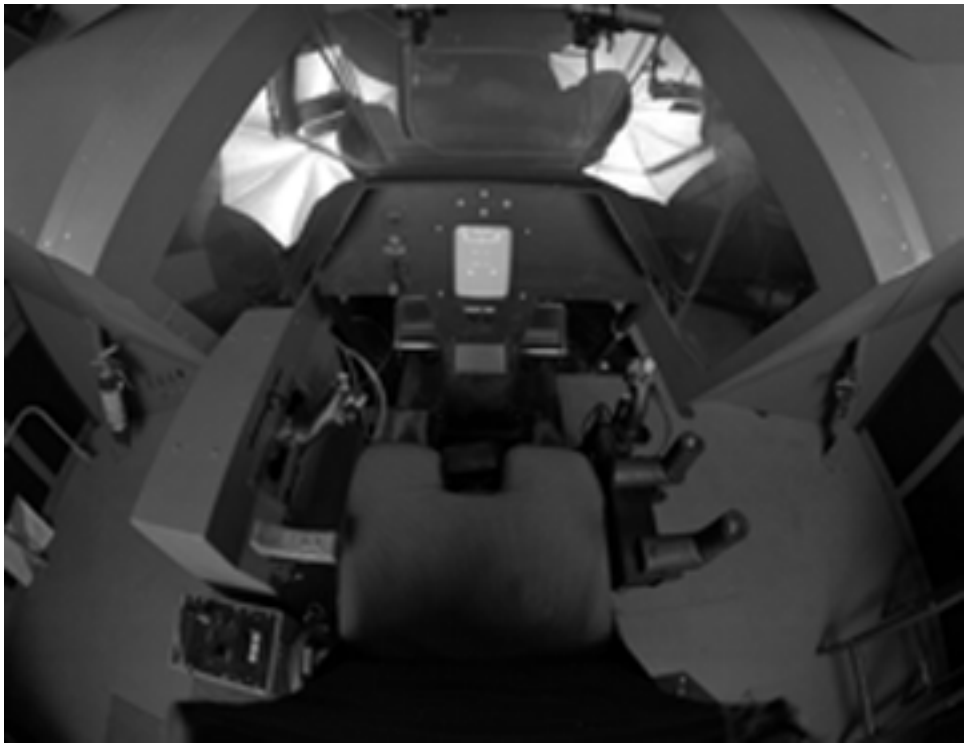

Figure 6. Simulator cockpit interior.

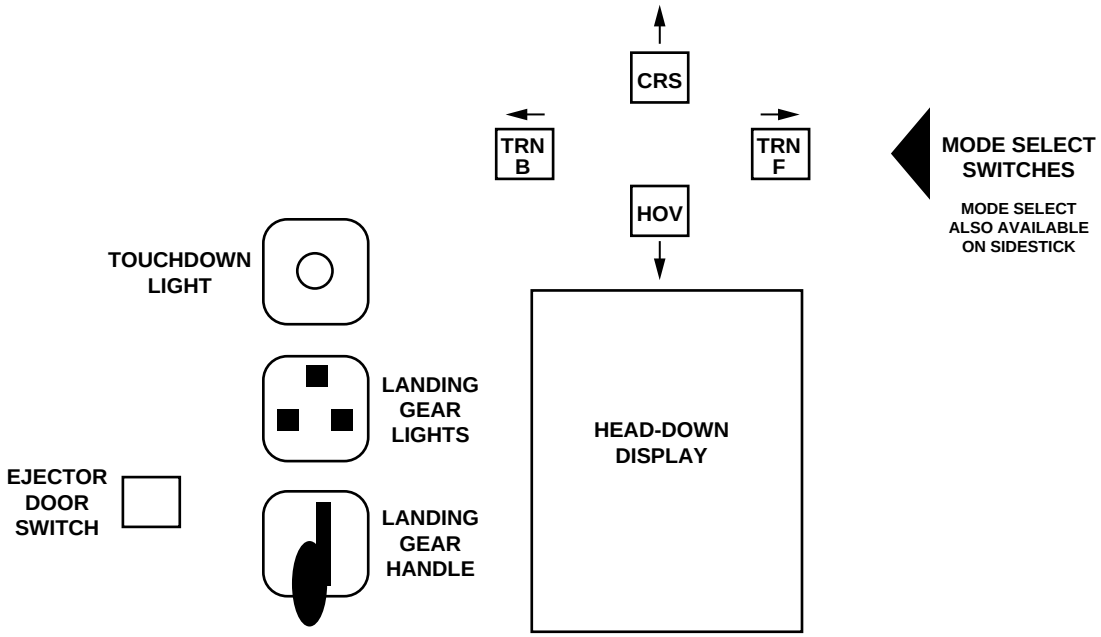

Figure 7. Instrument panel layout.

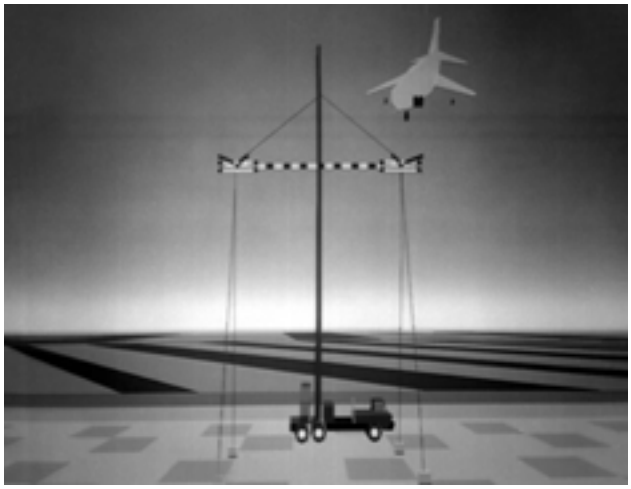

Lateral task

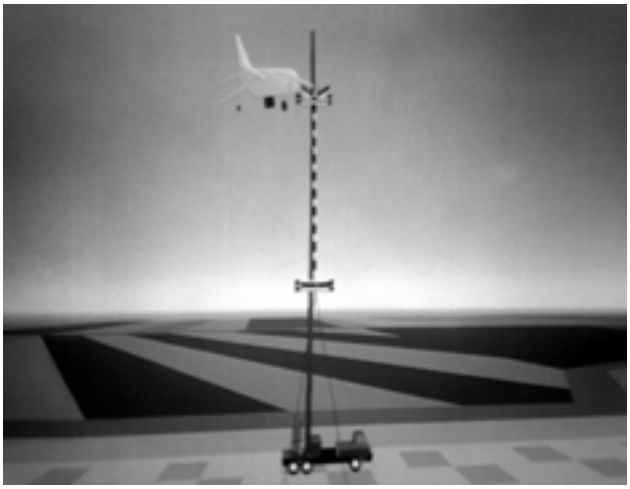

Vertical task

(a) Hover target arrangements

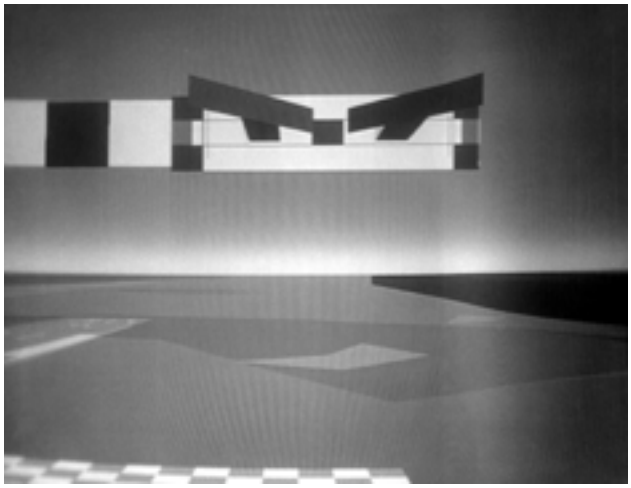

(b) Target close up

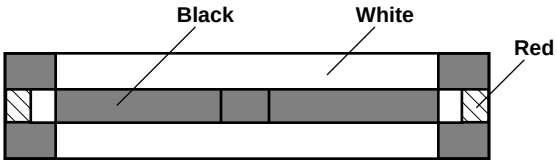

(c) Target appearance when in position

Figure 8. Precision hover target display.

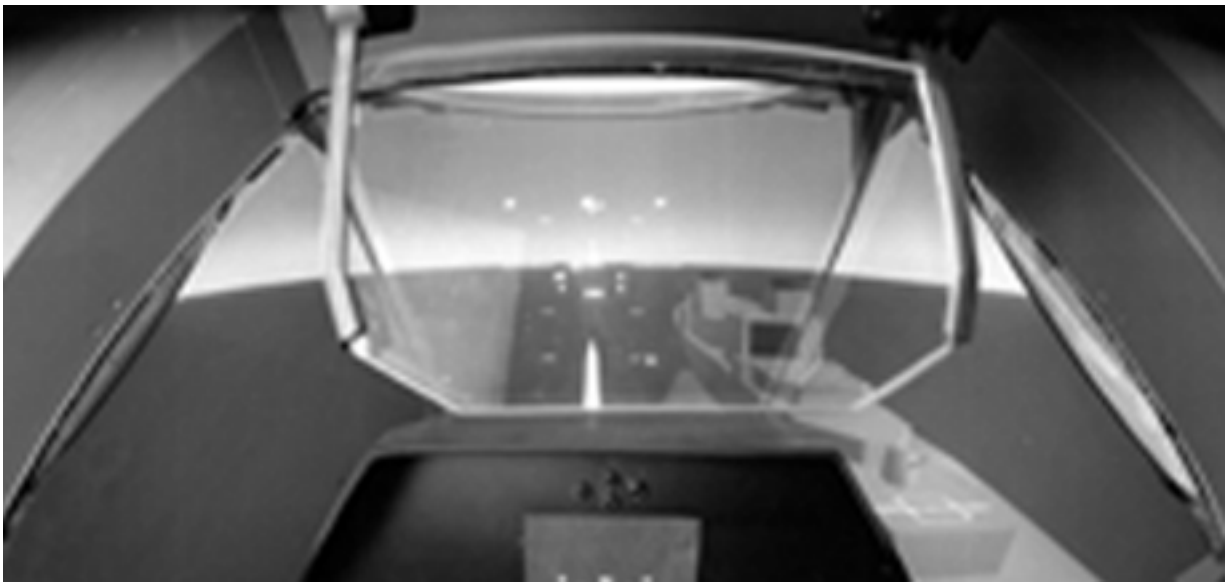

Figure 9. Small ship landing display.

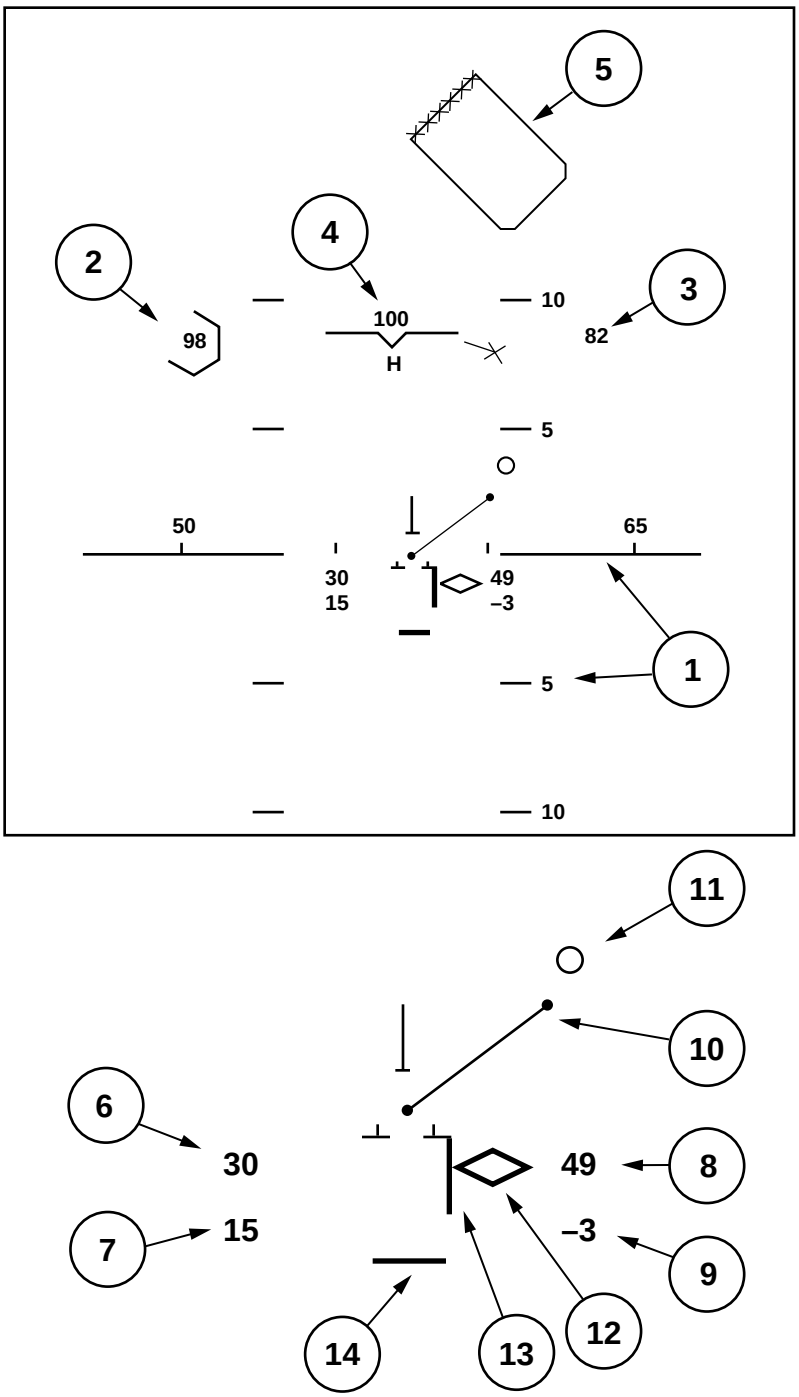

1. Horizon bar and pitch ladder
2. Engine (fan) percent RPM
3. Resultant thrust vector angle
4. Horizontal distance to touchdown point
5. Landing pad symbol
6. Airspeed
7. Ground speed
8. Height above ground/sea
9. Vertical velocity
10. Horizontal velocity vector
11. Horizontal velocity predictor ball
12. Vertical velocity predictor diamond
13. Allowable vertical velocity ribbon
14. Ground/deck bar

Figure 10. STOVL head-up display; hover mode.

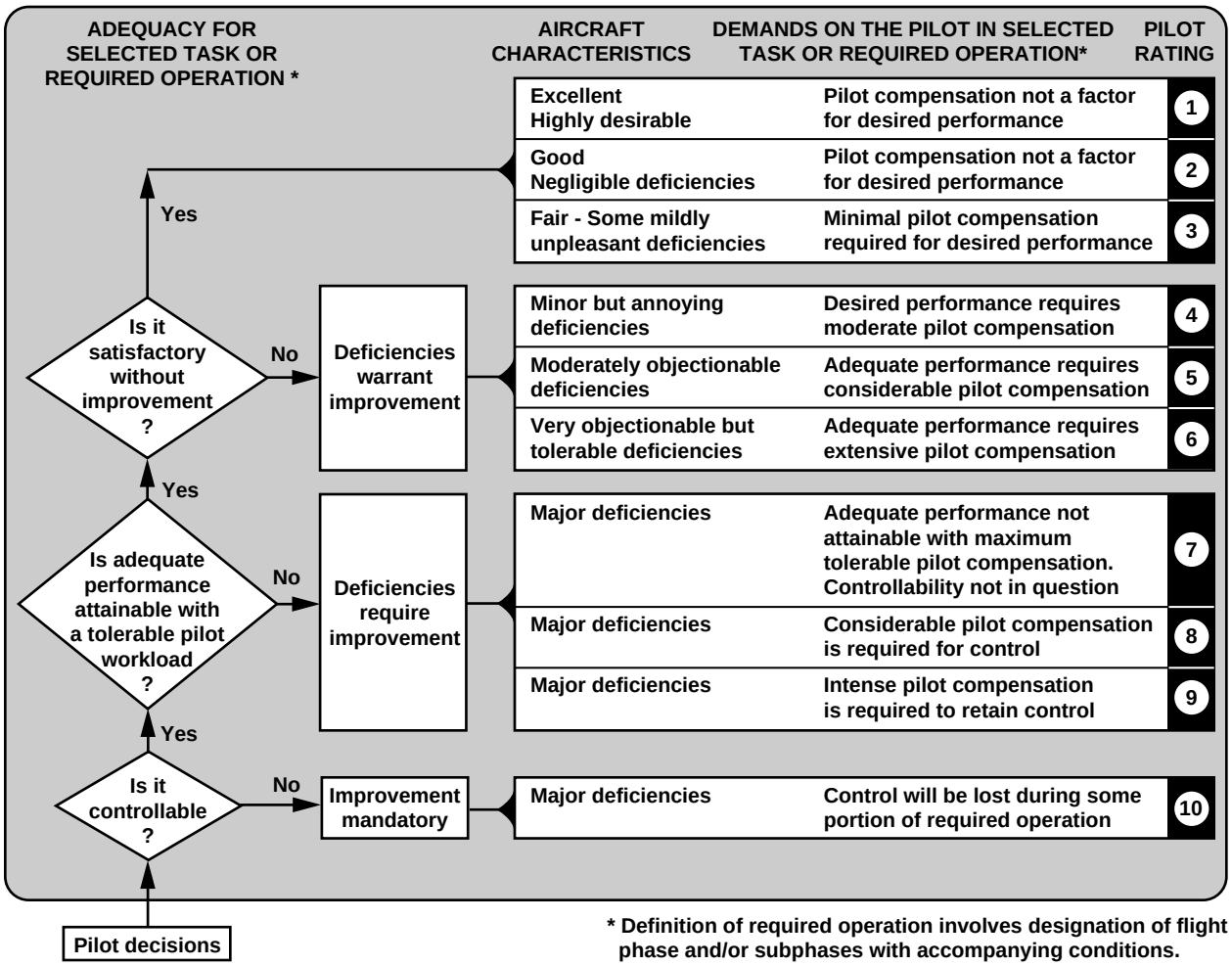

Figure 11. Handling-qualities rating scale.

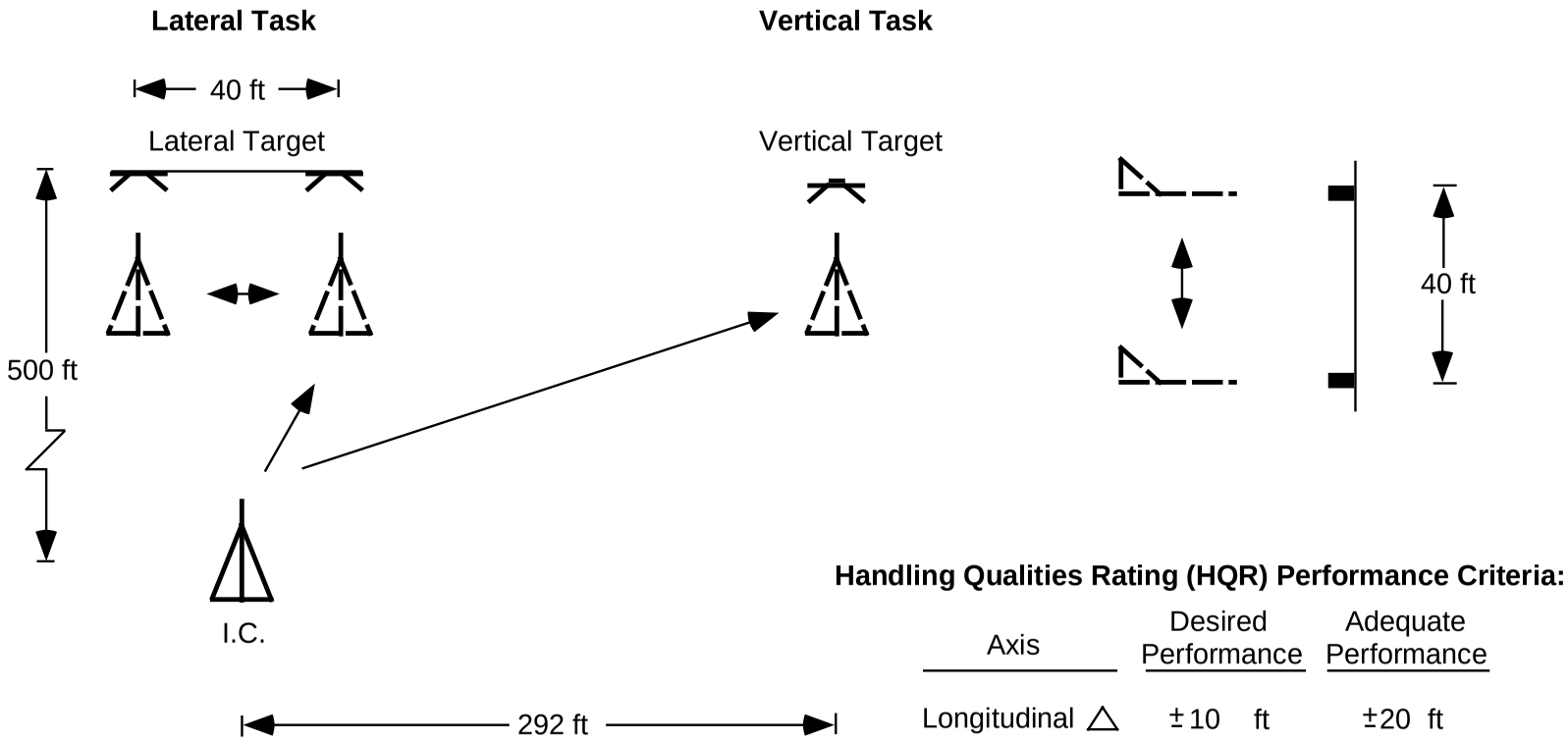

Handling Qualities Rating (HQR) Performance Criteria:

Axis	Desired Performance	Adequate Performance
Longitudinal △	±10 ft	±20 ft
Lateral △	± 5 ft	±10 ft
Vertical △	± 2.5 ft	± 5 ft

Figure 12. Lateral and vertical precision hover tasks.

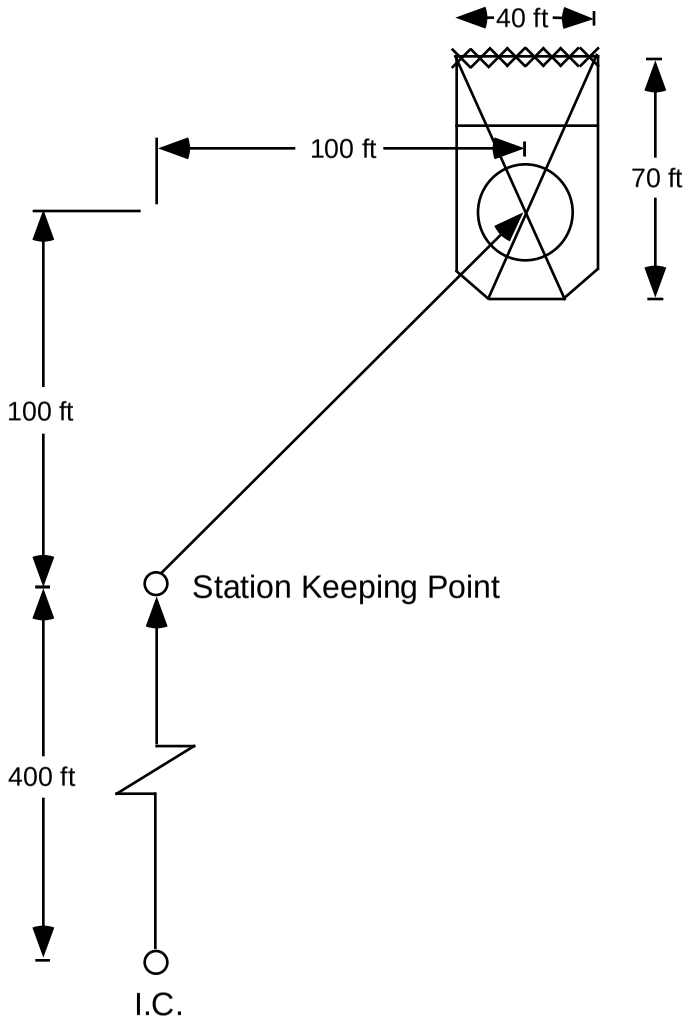

HQR Performance Criteria:

Axis	Desired Performance	Adequate Performance
Longitudinal △	± 2 ft	All three wheels within landing deck
Lateral △	± 2 ft	

Figure 13. Shipboard landing task.

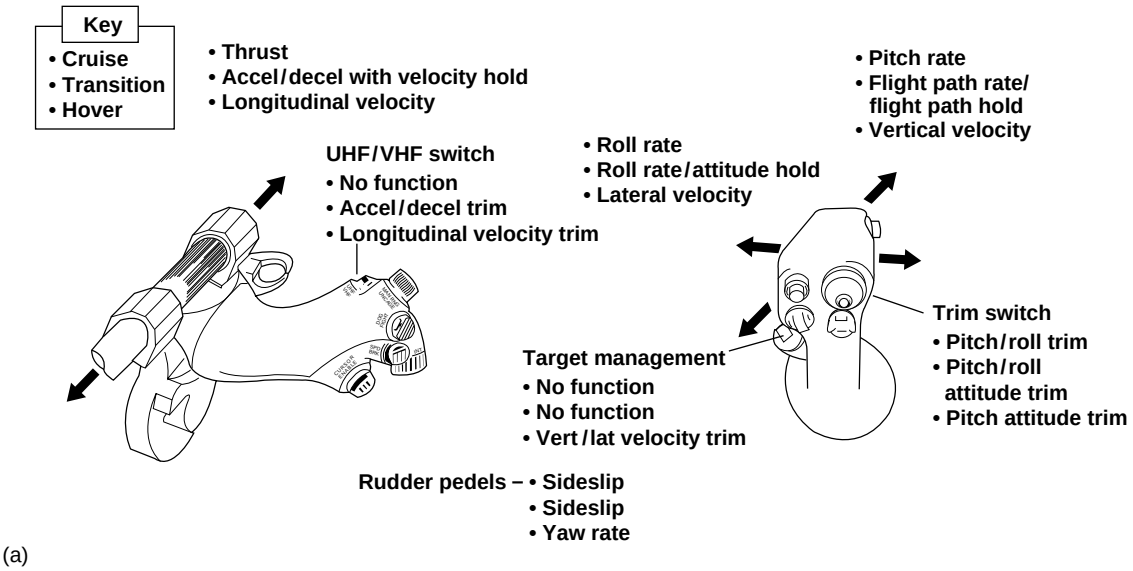

(a)

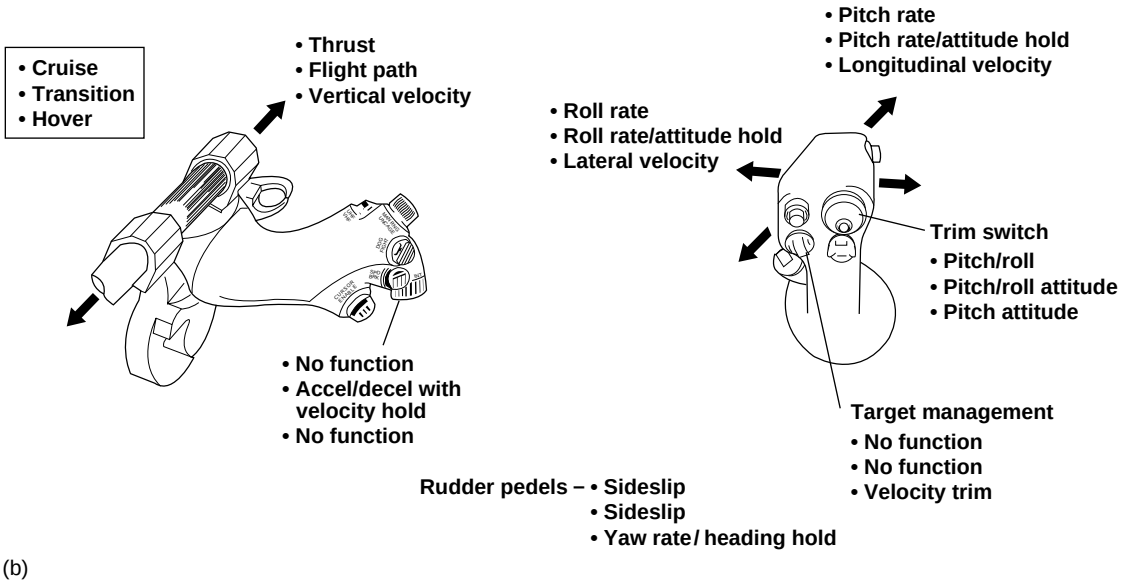

(b)

Figure 14. Control modes and inceptor configurations. (a) Front-side mode, (b) back-side mode.

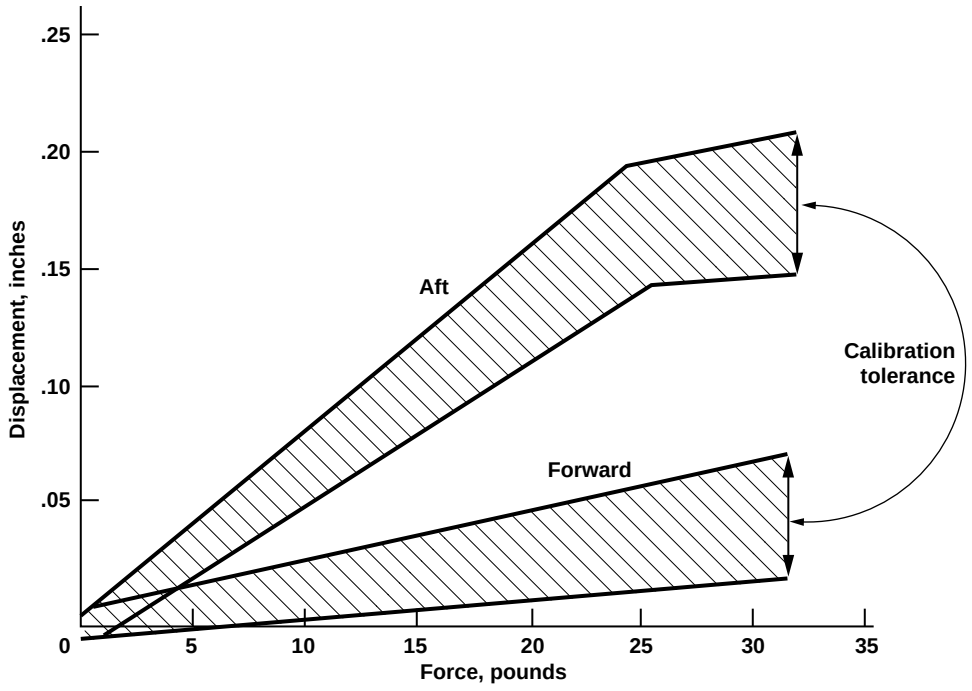

(a)

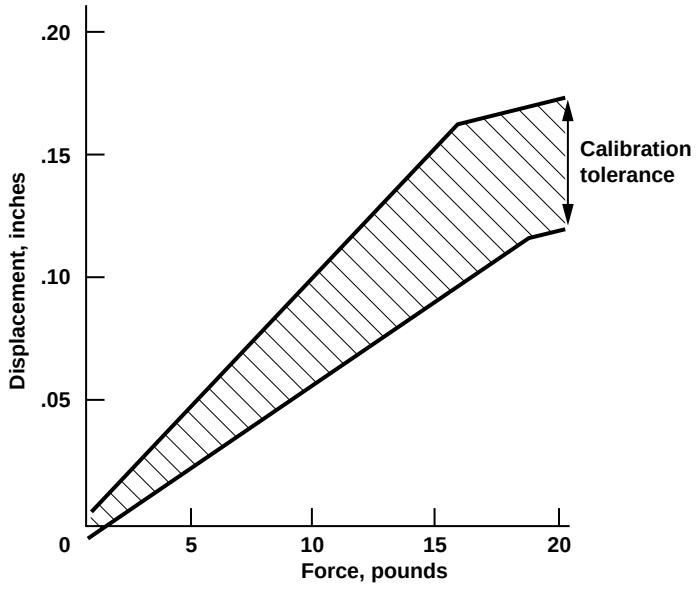

(b)

Figure 15. Right-hand controller-force gradients. (a) Longitudinal, (b) lateral.

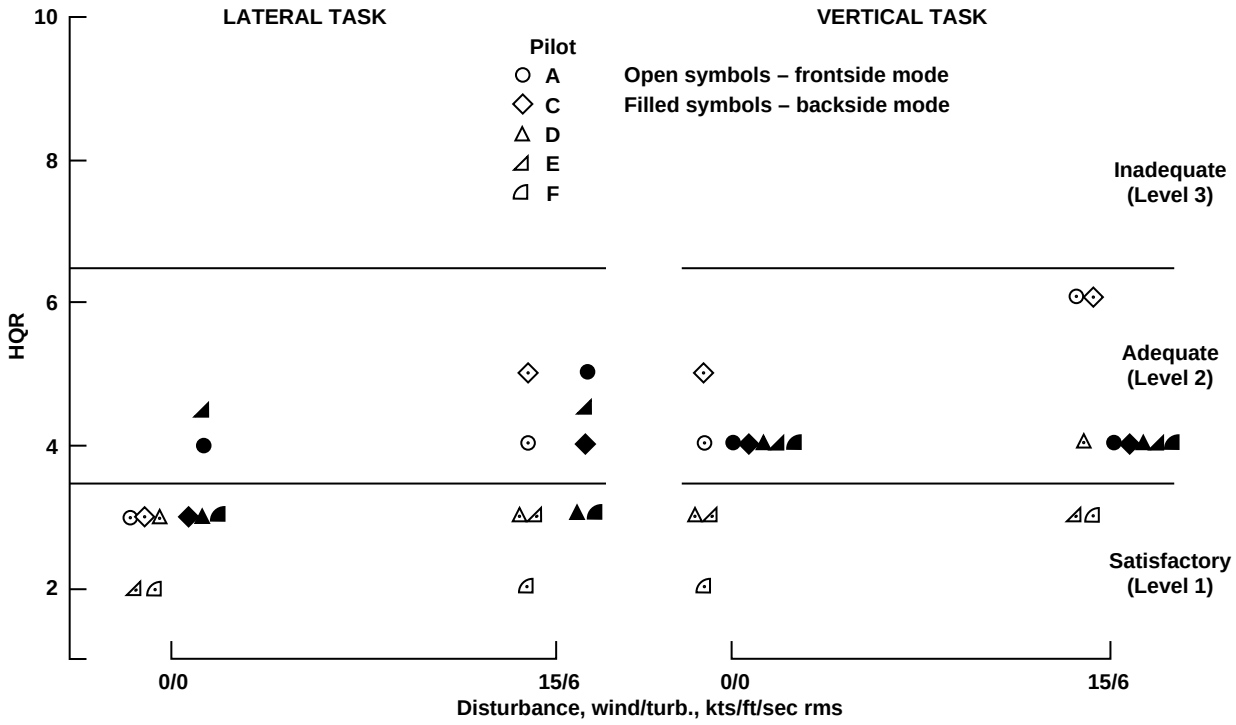

Figure 16. Handling-qualities ratings for precision hover tasks.

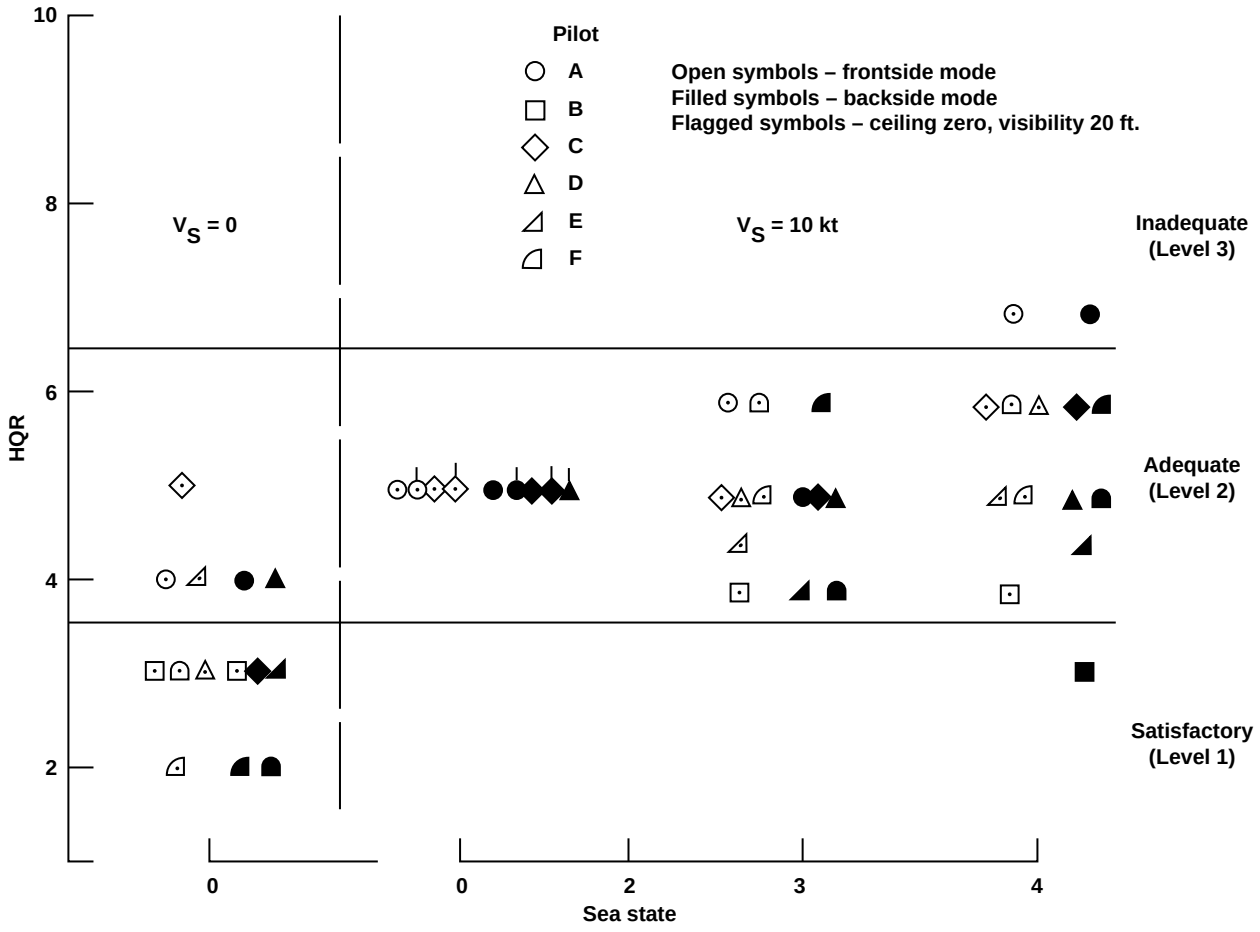

Figure 17. Handling-qualities ratings for the shipboard landing task.

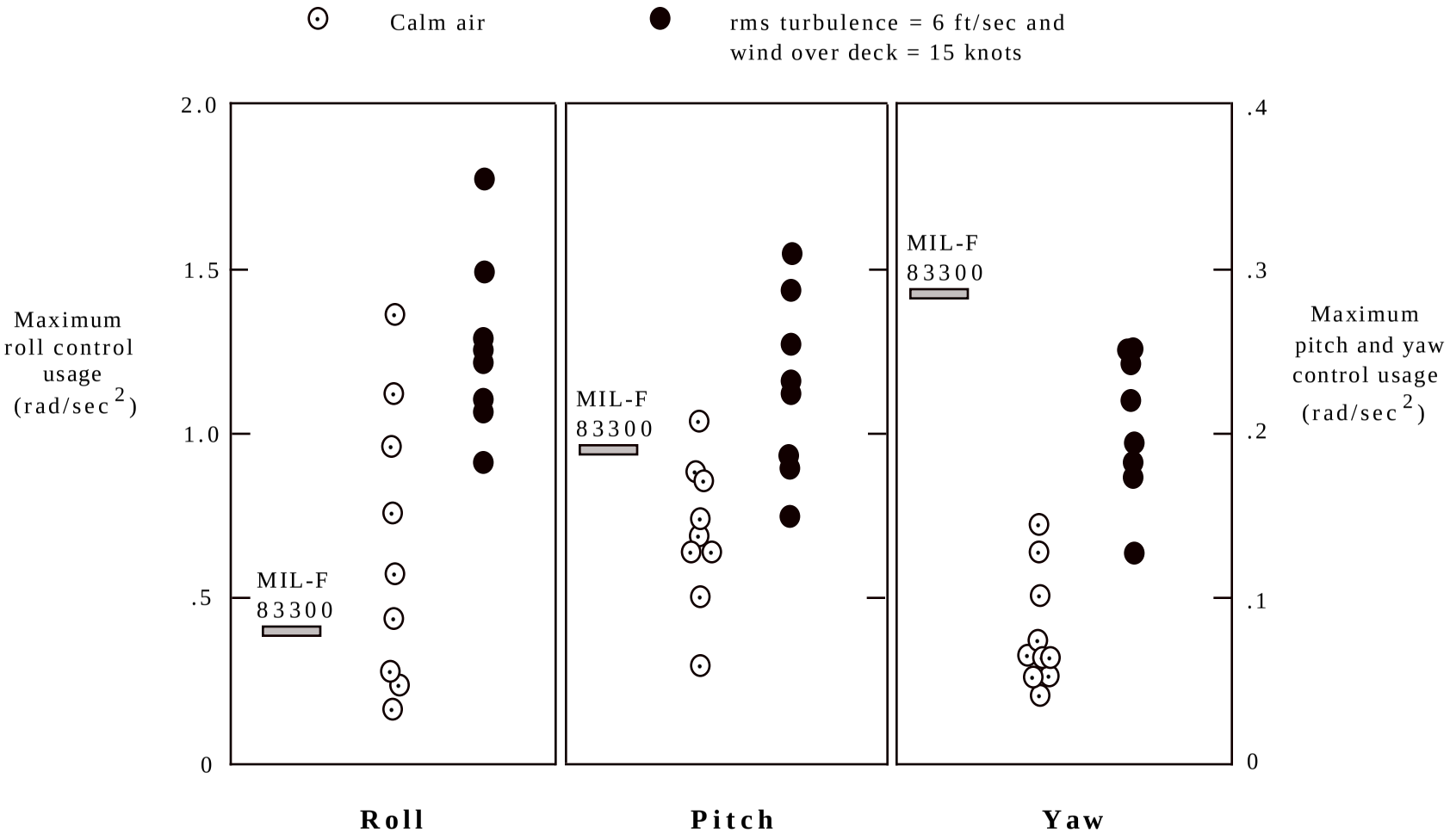

Figure 18. Influence on maximum control use in shipboard landings.

REPORT DOCUMENTATION PAGE

Form Approved
OMB No. 0704-0188

1. AGENCY USE ONLY (Leave blank)	2. REPORT DATE	3. REPORT TYPE AND DATES COVERED
	June 1995	Technical Memorandum

4. TITLE AND SUBTITLE

Moving Base Simulation of an Integrated Flight and Propulsion Control System for an Ejector-Augmentor STOVL Aircraft in Hover

5. FUNDING NUMBERS

505-68-32

6. AUTHOR(S)

Walter E. McNeill, William W. Chung, and Michael W. Stortz

7. PERFORMING ORGANIZATION NAME(S) AND ADDRESS(ES)

Ames Research Center
Moffett Field, CA 94035-1000

8. PERFORMING ORGANIZATION REPORT NUMBER

A-950046

9. SPONSORING/MONITORING AGENCY NAME(S) AND ADDRESS(ES)

National Aeronautics and Space Administration
Washington, DC 20546-0001

10. SPONSORING/MONITORING AGENCY REPORT NUMBER

NASA TM-108867

11. SUPPLEMENTARY NOTES

Point of Contact: William W. Chung, Ames Research Center, MS 243-5, Moffett Field, CA 94035-1000; (415) 604-1496

12a. DISTRIBUTION/AVAILABILITY STATEMENT

Unclassified-Unlimited
Subject Category – 05

12b. DISTRIBUTION CODE

13. ABSTRACT (Maximum 200 words)

A piloted motion simulator evaluation, using the NASA Ames Vertical Motion Simulator, was conducted in support of a NASA Lewis contractual study of the integration of flight and propulsion systems of a STOVL aircraft. Objectives of the study were to validate the Design Methods for Integrated Control Systems (DMICS) concept, to evaluate the handling qualities, and to assess control power usage. The E-7D ejector-augmentor STOVL fighter design served as the basis for the simulation. Handling-qualities ratings were obtained during precision hover and shipboard landing tasks. Handling-qualities ratings for these tasks ranged from satisfactory to adequate. Further improvement of the design process to fully validate the DMICS concept appears to be warranted.

14. SUBJECT TERMS	15. NUMBER OF PAGES
STOVL, Integrated flight/propulsion control system, DMICS	31
	16. PRICE CODE: A03

17. SECURITY CLASSIFICATION OF REPORT	18. SECURITY CLASSIFICATION OF THIS PAGE	19. SECURITY CLASSIFICATION OF ABSTRACT	20. LIMITATION OF ABSTRACT
Unclassified	Unclassified		

NSN 7540-01-280-5500

Standard Form 298 (Rev. 2-89)
Prescribed by ANSI Std. 239-18
298-102